Morphological Studies of Binary Mixtures of Block Copolymers. 1. Cosurfactant Effects and Composition Dependence of Morphology

François Court[†,‡,§] and Takeji Hashimoto[*,†]

Department of Polymer Chemistry, Graduate School of Engineering, Kyoto University, Kyoto 606-8501, Japan, and Laboratoire de Physico-Chimie Structurale et Macromoléculaire, ESPCI, 10 rue Vauquelin, 75005 Paris, France

Received July 25, 2000

ABSTRACT: The morphological behavior of a series of binary mixtures of polystyrene-*block*-polyisoprene (SI) diblock copolymers has been investigated by small-angle X-ray scattering and transmission electron microscopy. These mixtures consist of a given asymmetric SI diblock, coded *as*, which itself exhibits a morphology of polystyrene spheres on a body-centered-cubic lattice in a polyisoprene matrix and a symmetric SI diblock of lower molecular weight. This paper addresses the effect of varying the molecular weight of the symmetric diblock on the phase diagram of the binary blend. Three different short symmetric diblocks, coded s_1, s_2, and s_3, have been used. Their molecular weights are such that both s_1 and s_2 are in an ordered state at room temperature, exhibiting the lamellar morpology, while the shortest one, s_3, is in a disordered state. We show that over the whole composition range these binary mixtures do not undergo macrophase separation. The two types of chains self-organize in either a single ordered phase or a single disordered phase. We show that the phase diagram does not depend only on the overall volume fraction of both chemical species in the system, i.e., polystyrene and polyisoprene, but is also strongly affected by the ratio between the chain lengths of the asymmetric diblock and the symmetric diblock, $r = N_{as}/N_{s_i}$, where N_{as} and N_{s_i} are the degree of polymerizations of the asymmetric and symmetric diblock copolymers s_i ($i = 1$, 2, and 3), respectively. The effect of this parameter is a shift of the phase boundaries between neighboring morphologies. Therefore, blending diblocks of different lengths and compositions enables one to alter the relationship between thermodynamically stable morphology and volume fraction, which is not possible in single AB diblock systems alone. By analogy with surfactant systems and recent theoretical works of Shi and Noolandi, it can be described as a "cosurfactant effect": a small amount of a short symmetric SI effectively changes curvature of the domains formed by a long asymmetric SI.

I. Introduction

Block copolymers have attracted much interest from theoreticians and experimentalists as they represent ideal models for studying the self-organization of materials, melts, or solutions. A lot of efforts have been dedicated to the understanding of the phase behavior of A−B diblock copolymers and led to the construction of a phase diagram in terms of the composition of the diblock (usually expressed in terms of volume fraction of A or B) and χN, where χ is Flory's segmental interaction parameter and N is the total degree of polymerization of the diblock (the chain length).[1−6]

In this paper we focus on a series of binary mixtures of diblock copolymers $(A-B)_\alpha$ and $(A-B)_\beta$, both being comprised of polymers A and B but having different composition and/or molecular weight. Several fundamental questions arise concerning the self-organization of such systems. The thermodynamically stable morphology of a pure diblock is a consequence of the balance between two competing interactions: (i) short-range segmental interactions and (ii) long-range interactions involving conformations of A and B block chains and packing of these chains in the confined domain space. These competing interactions depend on the block lengths and their ratio, i.e., the composition of the diblock. In the case of the binary mixtures of block copolymers, the stable ordered structure depends also on the competing long-range interactions between $(A-B)_\alpha$ and $(A-B)_\beta$, which involves the following fundamental and intriguing question: Will it be favored that the two types of diblocks mix on a molecular level and self-organize in a single morphology with their chemical junctions uniformly mixed on the common interface? Or will they phase separate on a macroscopic scale, each type of diblock forming its own natural morphology? In this series of works we focus on the former case and address further questions about the characteristics of the resulting morphology and microdomains sizes.

When the two diblocks have similar molecular weights and compositions, their mixtures are naturally expected to be miscible and to show a single morphology with its domain size being scaled with an average molecular weight of the mixture.[7a,b] Let us now consider the case where the two diblocks differ in composition but still remain miscible at a molecular level. The morphology of a 50/50 mixture of two diblocks, polystyrene-*block*-polyisoprene (SI)[8,9] or polystyrene-*block*-polybutadiene (SB),[10] both diblocks in each blend having the same molecular weight but phase-inverted morphologies (polyisoprene (PI) or polybutadiene (PB) cylinders in a polystyrene (PS) matrix for the one and PS cylinders in a PI or PB matrix for the other), was found to have a lamellar morphology. As the overall composition in PI (or PB) and PS is symmetric, it does not seem surprising that the blend has a lamellar morphology. Spontak et al.,[11] Zhao et al.,[12] and Sakurai et al.[13] reported interesting morphological variations, including formation of the gyroid morphology, with change in the overall

† Kyoto University.
‡ ESPCI.
§ Present address: Centre d'Etude de Recherche et de Développement d'ATOFINA, 27470 Serquigny, France.
* To whom correspondence should be addressed.

10.1021/ma001314+ CCC: $20.00
Published on Web 03/17/2001

composition of one block induced by changing the blending composition of two diblocks. This partial literature survey would lead us to think that binary mixtures of diblocks (miscible at a molecular level) behave like pure AB diblocks: the morphology of the blend is controlled by the overall volume fraction of A. However, a more careful look reveals that some authors have encountered systems with unexpected morphological behavior.[14a]

One example can be found in the mixtures of the two SI diblocks,[14a] HK7 ($M_n = 3.19 \times 10^4$, $f_{PS} = 0.32$) and HS10 ($M_n = 8.14 \times 10^4$, $f_{PS} = 0.6$), both neat diblocks having a lamellar morphology. Here M_n is number-average molecular weight, and f_{PS} is volume fraction of PS block in SI. The average PS composition of these mixtures (ϕ_{PS}) varies from 0.35 to 0.55; therefore, according to the phase diagram of pure SI diblocks, one would expect that all the blends have a lamellar morphology. However, the results show that this is not the case. Some blends were found to have a cylindrical or bicontinuous morphology, although this unexpected morphological behavior was left unsolved. We note that this type of "anomaly" had been encountered even before the work described above but on different systems; Kraus et al.[15] studied several blends of star block copolymers containing the same overall volume fraction in PS ($\phi_{PS} = 0.25$). They showed that, depending on the molecular characteristics of the components, the blend had a lamellar morphology, though this morphology is not likely for this composition. They suggested that this effect could be attributed to the polydispersity in molecular weight distribution. In a sense, this effect is considered to be caused by blending of block copolymers.

The purpose of our paper is to clarify this anomalous point using model binary mixtures of diblocks and to try to answer the question: Is the morphology of a binary mixture of diblocks $(A-B)_\alpha/(A-B)_\beta$ controlled only by the overall volume fraction of A? This paper is divided in four sections. In the first one, we describe the characteristics of the four diblocks that have been used, one long asymmetric diblock, *as*, and three short symmetric diblocks, s_1, s_2, and s_3, that differ primarily by their molecular weights. In the following sections, the morphological study of a series of binary mixtures between *as* and each of the short symmetric diblocks is presented. This would allow to discuss morphology of the mixtures in the parameter space of ratio of degree of polymerization of two SI diblocks r and ϕ_{PS} and hence to discuss the effect of r on the morphology of the mixtures. How is the size of the microdomains affected by blending is another question, which is beyond the scope of this paper; this important question will be addressed in one of the companion papers.[16]

II. Experimental Methods

II.1. Samples. SI's were prepared by sequential living anionic polymerization with *sec*-butyllithium as an initiator and cyclohexane as a reaction solvent. For each synthesis a precursor sample was taken before the second-step polymerization of isoprene to determine the molecular weight of the polystyrene block by size exclusion chromatography. Table 1 summarizes the characteristics of the different diblocks synthesized. Figure 1 schematically highlights the difference in molecular weights of PS and PI in the block copolymers used in terms of the difference in the length of each straight line.

II.2. Film Specimens. The film specimens of neat SI diblocks and binary mixtures of diblocks were prepared in the same way: 10 wt % polymer solutions were obtained by dissolving the polymer(s) with toluene as a neutraly good solvent for both PS and PI blocks. The solution was stirred for 5 h and then placed in a Petri dish in a controlled atmosphere at 25 °C. The neat block copolymers as well as all their binary mixtures are in disordered homogeneous solutions at this polymer concentrations.[17] The slow evaporation process of the solvent lasted over 3 weeks. The films specimens were further dried at 80 °C under vacuum until constant weights were attained. Thickness of the cast films was ca. 400 μm.

Table 1. Characteristics of the SI Diblocks

code	$\bar{M}_n \times 10^{-3}$ [a]	HI[b]	$\bar{M}_{n,PS} - \bar{M}_{n,PI} \times 10^{-3}$ [c]	$N_{PS} - N_{PI}$[d]	N[e]	w_{PS}[f]	f_{PS}[g]
as	47.0	1.03	9.6−37.4	92−550	642	0.205	0.185
s_1	18.6	1.03	9.6−9.0	92−132	224	0.515	0.485
s_2	14.5	1.03	7.0−7.5	67−110	177	0.485	0.455
s_3	12.1	1.03	6.3−5.8	61−85	146	0.52	0.49

[a] $\bar{M}_n$: number-average molecular weight determined by size exclusion chromatography (SEC). [b] HI = $\bar{M}_w/\bar{M}_n$: heterogeneity index for molecular weight distribution. [c] $\bar{M}_{n,k}$: number-average molecular weight of the kth block (k = PS or PI). [d] N_k: number-average degree of polymerization of the kth block (k = PS or PI). [e] N: total number-average degree of polymerization of the diblock: $N = N_{PS} + N_{PI}$. [f] w_{PS}: polystyrene weight fraction. [g] f_{PS}: volume fraction of the PS block calculated from $f_{PS} = (w_{PS}/\rho_{PS})/(w_{PS}/\rho_{PS} + (1 - w_{PS})/\rho_{PI})$ by using the following densities for the PS and PI blocks, $\rho_{PS} = 1.0514$ g cm^{-3} and $\rho_{PI} = 0.925$ g cm^{-3}.

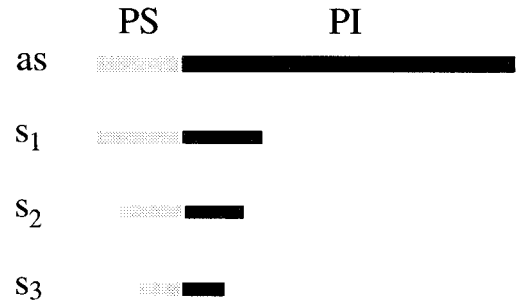

Figure 1. Schematic representation of the four SI diblocks investigated. The differences of molecular weight of the PS and PI block chains are intuitively shown schematically by the difference in their lengths of the straight lines.

II.3. Small-Angle X-ray Scattering. The microdomain structures were investigated by small-angle X-ray scattering (SAXS) using a rotating anode X-ray generator operated at 50 kV and 200 mA.[18−20] The X-ray is monochromated by a graphite crystal, and its wavelength corresponds to Cu Kα (λ = 0.154 nm). The scattered intensity is measured with a one-dimensional position-sensitive proportional counter placed at the end of a 1166 mm camera. The SAXS profiles were corrected for the air scattering, the absorption, the slit height, and slit width smearing effects.[18−21] The absolute SAXS intensity was determined by the Nickel foil method.[22] Each profile was recorded at room temperature over a period of 2 h. The profiles are represented as a function of magnitude of scattering vector, q, which is related to the scattering angle, θ, by eq 1:

$$q = (4\pi/\lambda)\sin(\theta/2) \quad (1)$$

The scattered intensity is represented on a logarithmic scale in arbitrary units.

II.4. Transmission Electron Microscopy. The microdomain structures were examined by transmission electron micoscopy (TEM). Ultrathin sections of 40−50 nm thickness were obtained from the film specimens using a Reichert ultramicrotom operated at −100 °C. The sections were then exposed to OsO_4 vapor for 1 h. This procedure is known to induce the selective staining and cross-linking of the double bonds of the polyisoprene with OsO_4.[23] The stained sections were observed with a Hitachi H-600S TEM operated at 100

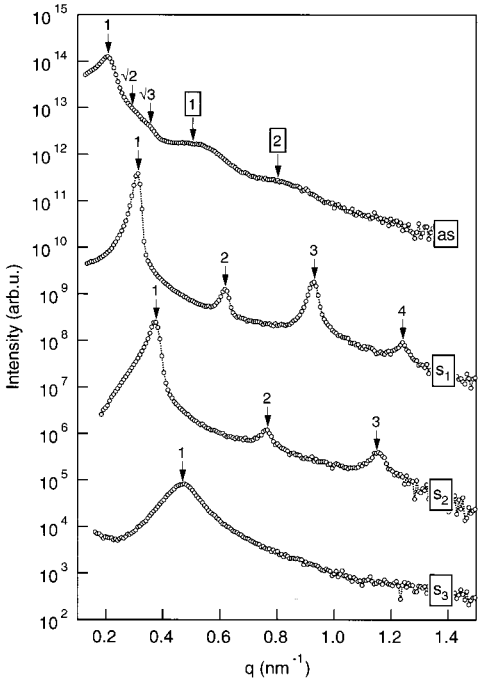

Figure 2. Small-angle X-ray scattering (SAXS) profiles of the neat SI diblocks (*as*, s_1, s_2, and s_3). The intensity (in arbitrary units) is shown on a logarithmic scale. The profiles have been shifted vertically for clarity.

keV. On the TEM pictures the PI microdomains appear dark, while the PS microdomains appear bright.

II.5. Optical Microscopy—Birefringence. The microdomain structures were also investigated by optical microscopy. The film specimen was placed in a conventional optical microscope between crossed polarizers. The observation was carried out under a ×10 objective lens. Some samples appeared completely dark, therefore nonbirefringent. Others revealed a mosaic of bright and dark areas of several microns, with no peculiar shape. The birefringence of block copolymer films has been studied by several authors.[24,25] The lamellar and cylinder morphologies have local optical anisotropy due to form birefringence[26] with their optical axes parallel to the lamellar normal or to the cylinder axis. Under crossed polarizers the grains of lamellae or cylinders appear bright or dark when their optical axes are inclined or parallel to one of the polarizer or analyzer axes, respectively.

III. Results and Discussion

III.1. Characterization of the Morphology of the Neat Diblock Copolymers. The SAXS profiles of the neat SI diblocks, *as*, s_1, s_2, and s_3, are represented in Figure 2. On each profile, the position of the first-order maximum can be easily determined. On the SAXS profiles of s_1 and s_2 we have indicated the positions of the higher-order scattering maxima by an arrow with number; the scattering maxima exist at integer multiples of the first-order peak position, indicating that the morphology of these samples is lamellar. The second-order SAXS peak of sample s_1 is relatively weak compared with the first- and third-order peaks. This is an indication that the alternating lamellae are of nearly comparable thicknesses. In fact, a more detailed analysis, which was carried out on sample s_1, using paracrystal analysis,[27] yielded a volume fraction of the minor component being 0.47, a value very close to the volume fraction f_{PS} of s_1. The SAXS profile of s_3 is significantly different from the profiles of the other two symmetric diblocks; it presents only one broad scattering maximum characteristic of a diblock in a disordered state. The molecular weight of s_3 is not large enough to segregate into the ordered lamellae above its glass transition temperature in disordered state (T_g) as elucidated elsewhere.[28] Film specimens of these three symmetric diblocks were observed under polarized optical microscopy. It revealed that s_1 and s_2 are birefringent, while s_3 is nonbirefringent. Such observations are consistent with the SAXS results.

The SAXS profile of *as* (Figure 2) shows the two shoulders at $q = q_m\sqrt{2}$ and $q = q_m\sqrt{3}$, where q_m is q at the first-order peak, indicating spheres in a cubic lattice as a possible morphology. Besides, the two broad peaks can be observed, as indicated by arrows marked by 1 and 2 in squares in Figure 2. They can be attributed to the maxima from the form factor. In the case of spheres a relation exists between an average radius of spheres, R, and the positions of the first-order and second-order maxima from the form factor with respect to q defined by q_{f1} and q_{f2}, respectively:

$$R = 5.765/q_{f1} = 9.10/q_{f2} \qquad (2)$$

It is then possible to calculate the volume fraction of PS spheres in the sample, $f_{PS,SAXS}$, assuming the symmetry of the lattice: $f_{PS,SAXS} = (4\pi/3)(R/D)^3$ for simple-cubic lattice (scc) or $(\sqrt{8}\pi/3)(R/D)^3$ for body-centered-cubic lattice (bcc) where $D = 2\pi/q_m$. By inserting $R =$ 12 nm estimated from eq 2 and $D = 30.8$ nm, $f_{PS,SAXS} =$ 0.25 for scc and 0.175 for bcc. The actual volume fraction of polystyrene in the sample ($f_{PS} = 0.185$ in Table 1) is much closer to the value obtained under the assumption of a bcc lattice than to the one obtained with a simple cubic lattice. This result suggests that the diblock *as* has a spherical morphology organized on a bcc lattice. A film specimen of *as* diblock observed under optical microscopy between crossed polarizers did not show birefringence, consistent with the SAXS analysis: As the bcc morphology is isotropic, it cannot give form birefringence.

A series of binary mixtures of the long asymmetric diblock, *as*, with each of the three short symmetric diblocks, s_1, s_2, and s_3, have been investigated. The results obtained are discussed in the following sections.

III.2. Morphological Study of *as*/s_1 Binary Mixtures. The compositions of the blends investigated are summarized in Table 2. SAXS profiles of five of the mixtures are represented in Figure 3. Besides the case of the mixture 64/36 which will be discussed later, it appears that each profile can be attributed to single well-known morphologies (Table 2). The SAXS signatures, together with the transparency of all the blends films, are strong indications that *as* and s_1 are miscible on a molecular level, forming ordered microdomain morphologies. The mixture 64/36 did not show birefringence, suggesting an optically isotropic morphology with no form birefringence.

In Figure 3, it is noted for the mixtures having a lamellar morphology that the first-order scattering maximum shifts toward smaller q when the fraction of *as* in the mixture increases, indicating that the lamellar spacing increases, when the long asymmetric diblocks are incorporated into the lamellar domains formed by the short diblock. A more detailed analysis of this phenomenon will be presented in the companion paper.[16] It should be also noted that the third-order peak is very weak compared with the second-order and fourth-order peaks for the 59/41 and 50/50 blends, indicating that the PS lamellae in these blends have a

Table 2. Characteristics of the Blends *as*/s_1, *as*/s_2, and *as*/s_3 Studied in This Work[a]

w_{as}/w_{s_1}[b]	n_{as}[c]	ϕ_{PS}[d]	morphology[e]	w_{as}/w_{s_2}[b]	n_{as}[c]	ϕ_{PS}[d]	morphology[e]	w_{as}/w_{s_3}[b]	n_{as}[c]	ϕ_{PS}[d]	morphology[e]
0/100	0	0.485	L	0/100	0	0.455	L	0/100	0	0.49	D
25/75	0.115	0.42	L	21/79	0.07	0.395	L	20/80	0.06	0.42	D
50/50	0.28	0.35	L	*35/65*	0.14	0.36	L	*35/65*	0.10	0.39	D
54/46	0.32	0.335	L	*45/55*	0.20	0.33	L	39/61	0.145	0.365	L
59/41	0.365	0.32	L	*54/46*	0.265	0.305	L	*45/55*	0.185	0.34	L
64/36	0.415	0.3	B	*60/40*	0.31	0.29	L	*55/45*	0.26	0.305	L
69/31	0.47	0.285	C	68/32	0.39	0.268	L	*68/32*	0.34	0.285	L
75/25	0.545	0.265	C	69/31	0.40	0.265	B	*71/29*	0.385	0.27	L
100/0	1	0.185	S	75/25	0.475	0.25	B	*75/25*	0.435	0.26	L
				79/21	0.54	0.235	C	78/22	0.485	0.245	L
				95/05	0.85	0.20	C	82/18	0.54	0.235	B
				100/0	1	0.185	S	*84/16*	0.59	0.23	B
								90/10	0.72	0.21	C
								97/03	0.90	0.195	C
								100/0	1	0.185	S

[a] The SAXS profiles were not shown in Figures 3, 4, and 6 for these blends with their blend compositions shown by italic numbers. [b] w_i: weight fraction of ith diblock in the blend ($i = as$, s_1, s_2, or s_3). [c] n_{as}: number fraction of the long asymmetric chains (*as*) in the blend. [d] ϕ_{PS}: volume fraction of PS in the blend calculated from the composition of the neat diblocks (w_{PS} in Table 1), blend composition, and densities of ρ_{PS} and ρ_{PI} in Table 1. [e] L, B, C, S, and D stand for lamellar, bicontinuous, hexagonal-cylinder and bcc-sphere morphology, and disordered state.

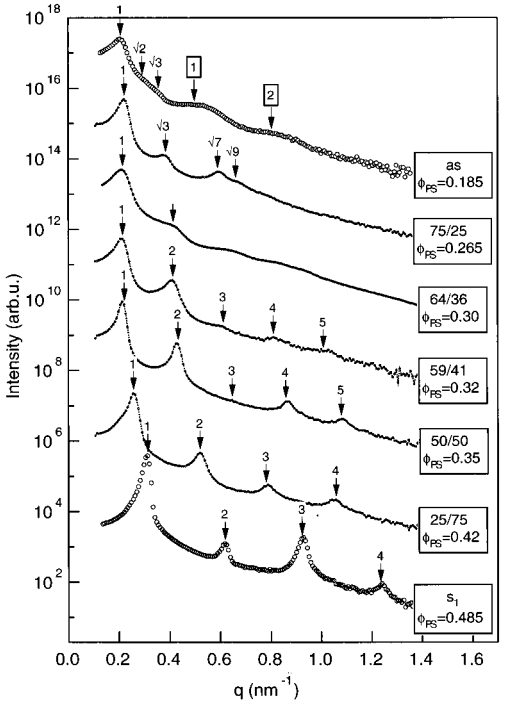

Figure 3. SAXS profiles of *as*/s_1 mixtures having various compositions (100/0, 75/25, 64/36, 59/41, 50/50, 25/75, 0/100). The composition of the blends, expressed in weight fraction of *as* and s_1, is indicated in the figure. The total volume fraction of polystyrene in the mixture, ϕ_{PS}, is also indicated in the figure. The numbers above the arrows indicate the position of the peak relative to the first-order scattering maximum. In addition, the numbers inside boxes indicate the maxima in the form factor from the isolated spheres.

volume fraction close to $^1/_3$, as will be also detailed elsewhere.[16]

III.3. Morphological Study of *as*/s_2 Binary Mixtures. The composition of the blends investigated are also summarized in Table 2. As in the previous series of blends, all film specimens were perfectly transparent.

The SAXS profiles of eight *as*/s_2 mixtures are presented in Figure 4 together with the profiles of the pure diblocks. As in the first series of mixtures, two kinds of morphologies (lamellae and cylinders) can be easily identified from the profiles as summarized in Table 2. Mixtures containing up to 68 wt % of *as* exhibit a well-ordered lamellar morphology. The lamellar spacing increases with the fraction of *as* in the mixture. Mixtures with compositions ranging from 79 to 95 wt % of *as* exhibit a cylindrical morphology. The film specimens corresponding to these two categories are all birefringent. The third-order peak is missing in the 45/55 blend because of the same reason as discussed in section III.2.

Table 3. Microdomain Characteristics of the Blends with Cylindrical Morphologies

blend	D (nm)[a]	D_I (nm)[b]	R (nm)[c]	$\phi_{PS,SAXS}$[d]	$\phi_{PS,comp}$[e]
as/s_2 (79/21)	28.6	33	8.4	0.24	0.235
as/s_3 (90/10)	29.6	34.2	8.2	0.21	0.21

[a] D: Bragg spacing, $D = 2\pi/q_m$, where q_m is the wavenumber of the first-order scattering peak. [b] Interdomain distance: $D_I = (4/3)^{1/2}D$ for a hexagonal lattice. [c] Cylinders radius calculated from eq 3. [d] $\phi_{PS,SAXS}$: volume fraction occupied by the cylinders as calculated from the SAXS data; $\phi_{PS,SAXS} = (\sqrt{3}/2)\pi(R/D)^2$. [e] $\phi_{PS,comp}$: volume fraction of PS calculated from the composition of the pure diblocks and the composition of the blend, based on the assumption of a strong segregation that the PS and PI blocks completely segregate into their own domains.

The samples with intermediate compositions of *as*/s_2, 69/31 and 75/25, are nonbirefringent. However, they are in an ordered state as evidenced by the higher-order scattering maxima observed on their SAXS profiles (Figure 4b), and their ordered morphology will change into either lamellar or cylindrical morphology upon slightly increasing or decreasing fraction of s_2, respectively (see Table 2). TEM micrographs of the two mixtures *as*/s_2-69/31 and *as*/s_2-75/25 are represented in parts a and b of Figure 5, respectively. The morphology cannot be clearly ascertained from the micrographs, though it is neither lamellar nor cylindrical. It appears that the PS domains (appearing in bright in the micrograph) are interconnected in the three dimensions in the matrix of the PI domains, consistent with the fact that polystyrene is the minor component in this mixture ($\phi_{PS} = 0.25$). It is therefore very likely that the morphology is bicontinuous.[29] The bicontinuous morphology is consistent with the optically isotropic characteristic found for this blend.

III.4. Morphological Study of *as*/s_3 Binary Mixtures. This third series of blends presents a singularity compared with the two previous ones. The short symmetric diblock s_3, due to its low molecular weight, does not have a lamellar morphology above its T_g; it is in a

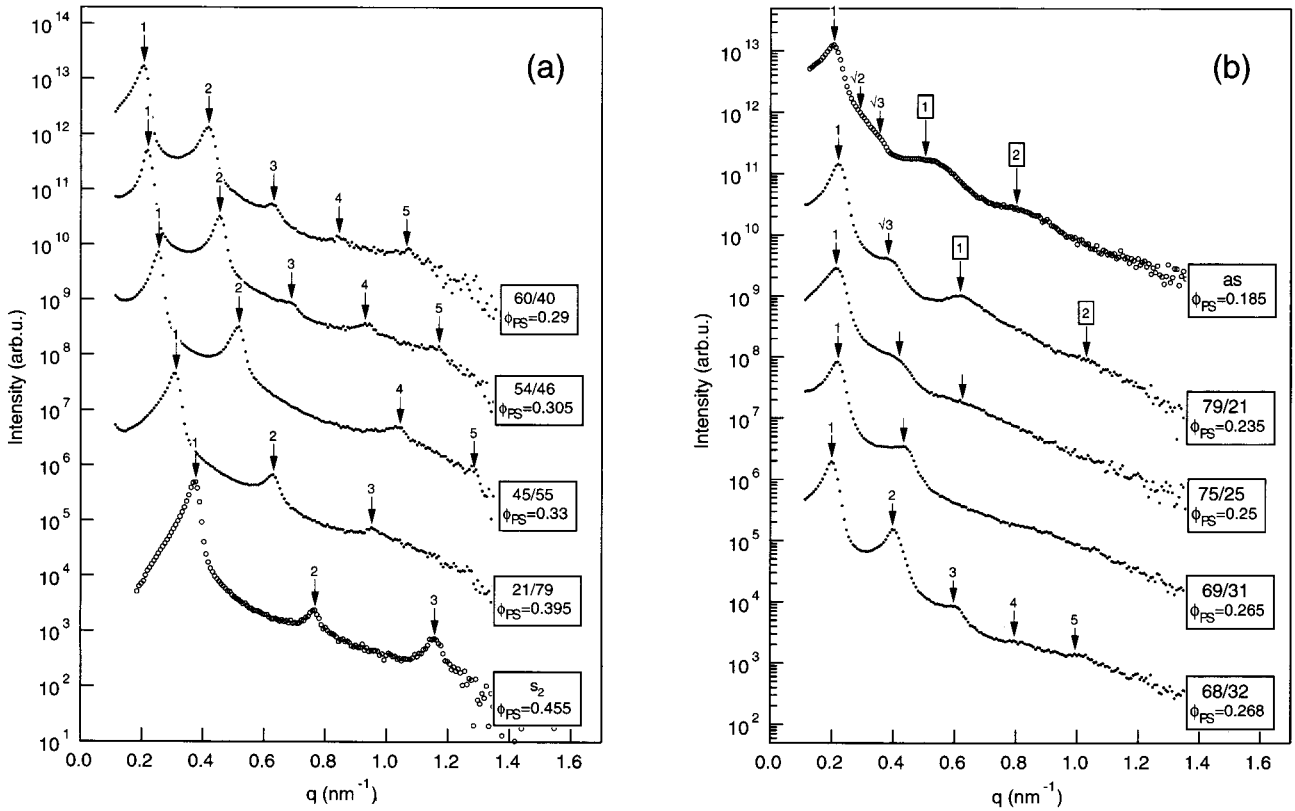

Figure 4. SAXS profiles of as/s_2 mixtures having various compositions ((a) 60/40, 54/46, 45/55, 21/79, 0/100; (b) 100/0, 79/21, 75/25, 69/31, 68/32). The composition of the blends, expressed in weight fraction of *as* and s_2, is indicated in the figure. The total volume fraction of polystyrene in the mixture, ϕ_{PS}, is also indicated in the figure. The numbers above the arrows indicate the position of the peak relative to the first-order scattering maximum. In addition, in part b the numbers inside boxes indicate the maxima in the form factor from the isolated spheres or cylinders.

disordered state. This raises an interesting question concerning the distribution of the short diblocks in the blend, as was addressed in the literature:[30,31] will s_3 junctions segregate at the interface created by the long asymmetric diblock, or will the s_3 diblock remain nonsegregated and swell the microdomains of *as* like an homopolymer of short molecular weight? In that case, will it swell preferentially the PS domains of *as* or the PI domains or both?

The compositions of the blends investigated are again summarized in Table 2. As in the previous series of blends, all film specimens were perfectly transparent. The SAXS profiles of nine as/s_3 mixtures are presented in Figure 6 together with the profiles of the pure diblocks. Let us first focus on the blend $as/s_3 = 20/80$. Its SAXS profile is characteristic of a disordered system. The broad scattering maximum corresponds to the correlation hole.[5] Comparing this profile with the profile of the pure s_3 diblock, it can be noted that the peak maximum is strongly shifted toward smaller q. This indicates that the wavelength of dominant modes of the concentration fluctuations increases when a small amount of the long *as* diblocks are added to the short s_3 diblocks. It is a clear evidence that the two types of chains, s_3 and *as*, are miscible at a molecular level. We can say that in this blend the short diblocks behave as a neutrally good solvent or as a plasticizer; it apparently reduces the segregation power, preventing the *as* chains from forming an ordered morphology. This dilution effect has been reported before.[32c]

By increasing the fraction of long chains in the blend, the segregation power increases and the blend becomes ordered. We found that the blends exhibit a lamellar morphology between 39% and 78% of *as* diblocks and a cylindrical morphology between 90% and 97% of *as* diblocks.

Figure 7 represents a TEM micrograph of the blend as/s_3-75/25. Interestingly enough, it demonstrates how the lamellar morphology with long-range order can be obtained by blending a diblock of the bcc spherical morphology with a disordered diblock. In this micrograph, the PS lamellae (bright phases) appear thinner than the PI lamellae (dark phases) as one would expect considering the asymmetric composition of this blend ($\phi_{PS} = 0.26$). In fact, the fourth-order peak is missing in the SAXS profile from this blend (Figure 6b), indicating that the PS lamellae have a volume fraction close to $^1/_4$, as expected from the overall composition $\phi_{PS} = 0.26$ and as will be detailed elsewhere.[16]

Over the composition range between lamellae and cylinders (e.g., the 82/18 and 84/16 blends in Table 2), the blends are nonbirefringent although they are in ordered state as evidenced by the higher-order SAXS maxima (Figure 6b). A TEM micrograph of one of those blends, $as/s_3 = 82/18$, is represented in Figure 8. It cannot be misinterpreted for lamellae or cylinders. This morphology is expected to be bicontinuous,[29] very similar to the one of the blend $as/s_2 = 75/25$ (Figure 5b). To illustrate the difference between this bicontinuous morphology and the cylindrical morpholgy, a TEM micrograph of the blend $as/s_3 = 90/10$ is given in Figure 9. The hexagonal lattice appears clearly in this figure. Figures 7−9 clearly indicate a trend for morphological transition with a small change of the blend composition w_{as}/w_{s3}.

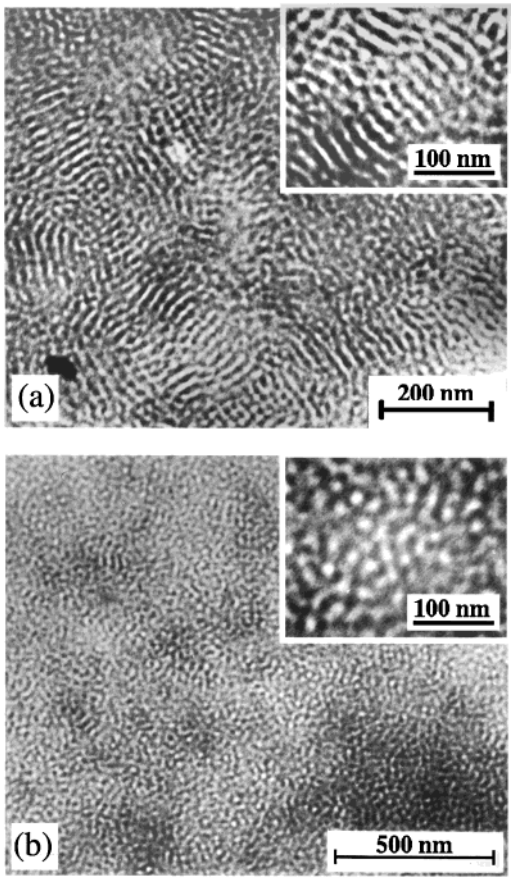

Figure 5. TEM micrographs for (a) the as/s_2 69/31 blend and (b) the as/s_2 75/25 blend.

IV. Further Discussion

IV.1. SAXS Analysis on the Characteristics of Cylindrical Morphologies. In the series of binary mixtures investigated, several blends showed a cylindrical morphology. Among them, two blends, $as/s_2 = 79/21$ and $as/s_3 = 90/10$, have SAXS profiles on which the scattering peaks from form factor can be detected. Although those peaks are not very intense, it enables us to estimate the radii of the cylinders R from the q value at the first-order and second-order scattering maxima from the form factor q_{f1} and q_{f2}, respectively, using eq 3 below and therefore the volume fraction that they occupy. The volume fraction thus estimated can be compared with that estimated from the blend composition and the block copolymers used for the blends, which yields a useful piece of information concerning the segregation between the PS and PI blocks in the ordered phase.

$$R = 4.98/q_{f1} = 8364/q_{f2} \quad \text{for cylinders} \qquad (3)$$

The results obtained are reported in Table 3 together with the total volume fraction of PS in the blend, $\phi_{PS,comp}$, calculated from the composition of the blend. This evaluation assumes that the two diblocks segregate with their chemical junctions on the same interface and that PS and PI blocks completely segregate into the respective domains. It appears, in both cases, that the volume fraction occupied by the cylinders, determined by the analysis of the SAXS profiles, $\phi_{PS,SAXS}$, is in a close agreement with $\phi_{PS,comp}$. This result is therefore consistent with the assumption that the PS and PI block chains are in a strong segregation and the chemical junctions of the two diblocks segregate on the same interface. It should be noted that the same conclusion is valid for the blends showing the lamellar morphology, as they also show $\phi_{PS,SAXS} = \phi_{PS,comp}$.

The radius of the cylinders of the blend $as/s_3 = 97/03$ cannot be unequivocally determined from its SAXS profile (Figure 6) though this sample is worth being investigated. One can notice that the addition of 3% of short symmetric diblock to *as* is enough to induce a morphological transition from the bcc sphere to the hexagonal cylinder. Two interpretations can be proposed to explain this morphological transition: either the short s_3 diblock swells preferentially the PS spherical domains of the long asymmetric diblock as a homopolystyrene (HS) of low molecular weight would do (wet brush regime) in the mixture of SI/HS; or the short and the long diblocks segregate with their chemical junctions on the same interface and with the two block chains segregating into their own domains, and the presence of short chains induces a change in the spontaneous curvature of the interface of *as*. The first explanation seems very unlikely as the short diblock has a symmetric composition ($\phi_{PS} = 0.49$). The reason why we consider that it might swell preferentially the PS domains rather than the PI domains is because the PS block of *as* is much shorter than its PI block. The first explanation is unlikely from the evidence clarified above in relation to $\phi_{PS,SAXS} = \phi_{PS,comp}$ as well.

The whole results clearly evidence that, in the three series of binary mixtures $(A-B)_\alpha/(A-B)_\beta$ investigated, the symmetric diblocks (s_1, s_2, and s_3), though they differ in molecular weight and in composition, are miscible with *as* on a molecular level. Furthermore, the morphological analysis conducted by SAXS clarifies the spatial distribution of the two types of diblocks *as* and s_i ($i = 1$, 2, 3): The PS and PI blocks segregate in their own domains with their chemical junctions of the short symmetric diblocks and of the long asymmetric diblocks on the same interface, except for the case of as/s_3-20/80 and -35/65 blends, which shows a single-phase and disordered state (Table 2).

IV.2. Characteristics of the Blends with Bicontinuous Morphologies. SAXS analysis left one point unclear, concerning the identification of the morphology-(ies) of the blends that are neither lamellar nor cylindrical. They have the common characteristics that their compositions lie in between the limits of the compositions for the lamellar and the cylindrical morphologies and that they are nonbirefringent. TEM observations clearly suggest that all those blends have morphology of neither lamellae nor cylinders and have a similar bicontinuous morphology where the PS domains are interconnected in 3D space and dispersed in the matrix of the PI domains (more or less interconnected cylinder morphology). In Figure 10 are presented the SAXS profiles of three blends $as/s_1 = 64/36$, $as/s_2 = 75/25$, and $as/s_3 = 82/18$. The SAXS profiles have been corrected for the smearing effects, and they are represented as a function of q/q_m and shifted vertically by a factor of 8 for the sake of clarity. A strong similarity is observed between the three profiles. The slight differences appearing at high q/q_m can be attributed to differences in the form factor scattering as these samples have significantly different compositions (ϕ_{PS}). Nevertheless, it can be concluded that these samples present a similar morphology. The second-order peak is found for $q/q_m = 1.9$, which does not correspond to the bicontinuous gyroid recently identified by Hajduk et al.[25] nor to the

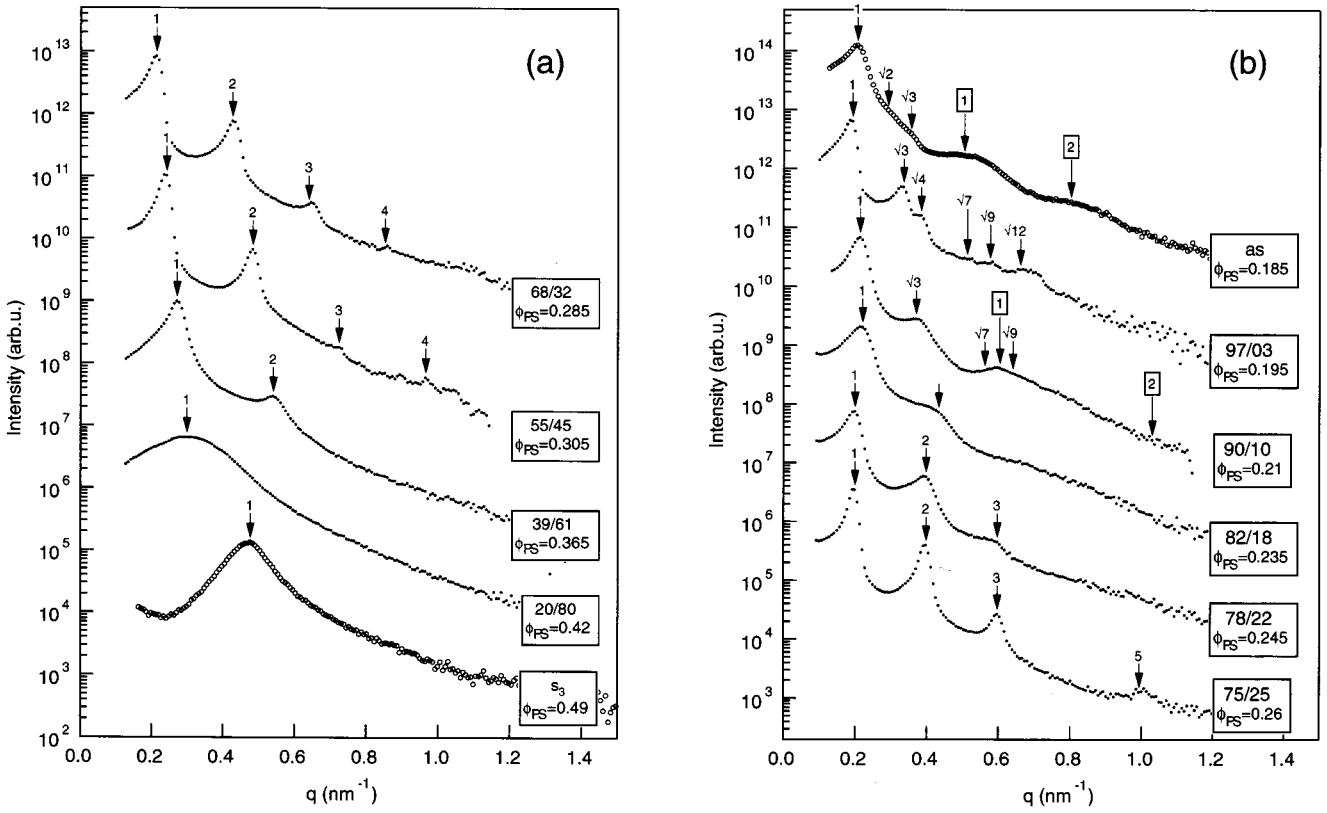

Figure 6. SAXS profiles of as/s_3 mixtures having various compositions ((a) 68/32, 55/45, 39/61, 20/80, 0/100; (b) 100/0, 97/03, 90/10, 82/18, 78/22, 75/25). The composition of the blends, expressed in weight fraction of *as* and s_3, is indicated in the figure. The total volume fraction of polystyrene in the mixture, ϕ_{PS}, is also indicated in the figure. The numbers above the arrows indicate the position of the peak relative to the first-order scattering maximum. In addition, in part b the numbers inside boxes indicate the maxima in the form factor from the isolated spheres or cylinders.

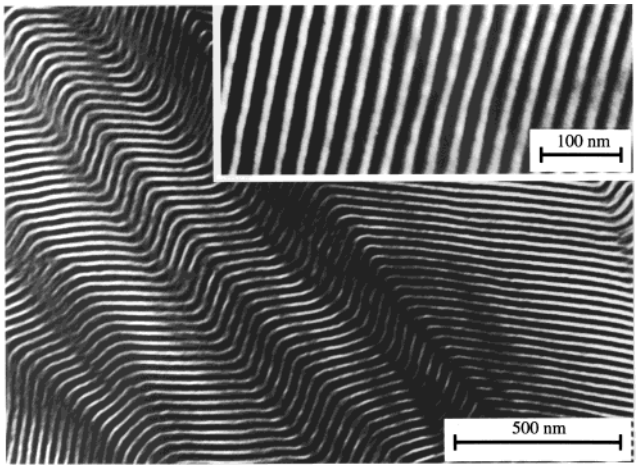

Figure 7. TEM micrograph for as/s_3 75/25 blend.

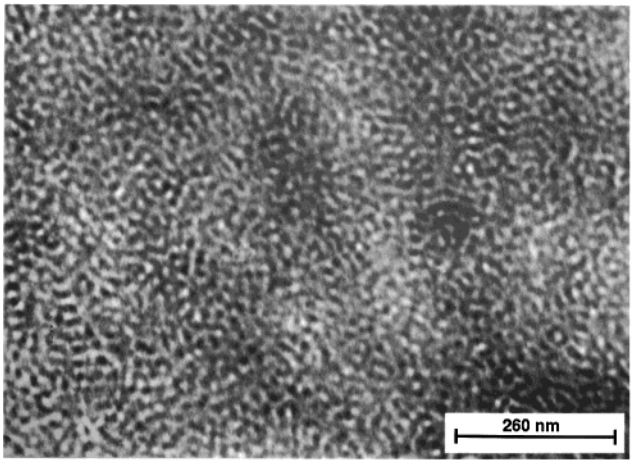

Figure 8. TEM micrograph for as/s_3 82/18 blend.

OBDD,[33–35] as the expected SAXS signatures of these morphologies are the Bragg reflections at $1:\sqrt{4/3}:\sqrt{7/3}:\sqrt{8/3}:\sqrt{10/3}:\sqrt{11/3}:\sqrt{13/3}:\sqrt{5}:\sqrt{16/3}$ and $1:\sqrt{3/2}:\sqrt{2}:\sqrt{3}:2:\sqrt{9/2}:\sqrt{5}:\sqrt{11/2}:\sqrt{6}$, respectively. This result is puzzling because in the case of pure diblocks it is now well established that one encounters the bicontinuous gyroid morphology in between the limits of the lamellar and the cylindrical morphologies.

To ascertain the symmetry of this morpholgy, the samples were annealed for a long period of time at elevated temperatures. However, we cannot obtain an improved order. It might require for future work to try to apply shear to the samples as it has been shown to increase the long-range order,[36] thus improving the accuracy of the SAXS profile. In the following sections we will refer to this morphology as bicontinuous, though its symmetry remains unidentified.

IV.3. Morphology Variations in the Parameter Space of *r* and ϕ_{PS}. The morphological study reported in earlier sections revealed that the morphologies of the different series of binary mixtures as/s_i (i = 1, 2, 3) investigated fall into five categories: disordered, lamellar, bicontinuous, cylindrical, and spherical. The large number of samples studied enables to determine accurately the limits of the different morphologies in terms of ϕ_{PS}, the total volume fraction of PS as summarized in Table 4. It appears that the composition range for

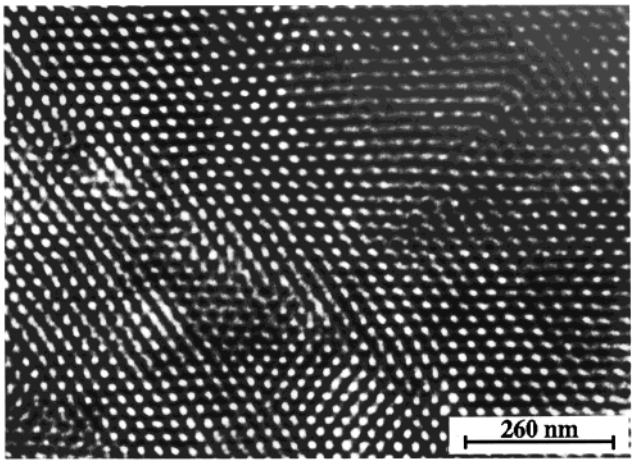

Figure 9. TEM micrograph for as/s_3 90/10 blend.

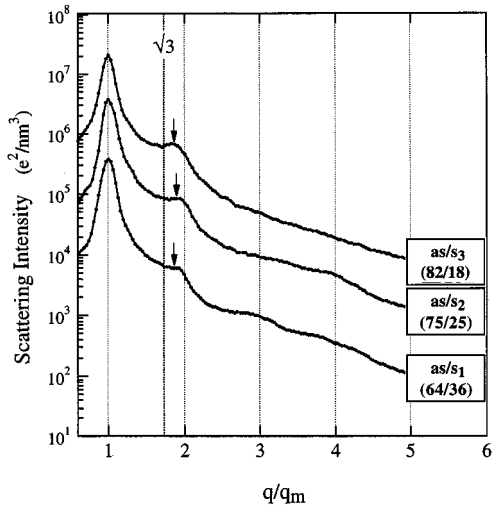

Figure 10. SAXS profiles of different as/s_i mixtures, showing the unidentified bicontinuous morphology. The composition of the blends, expressed in weight fraction of *as* and s_i (i = 1, 2, and 3), is indicated in the figure.

Table 4. Composition Limits between Lamellar and Bicontinuous Morphologies ($\phi_{Lam,Bic}$) and between Bicontinuous and Cylindrical Morphologies ($\phi_{Bic,Cyl}$) Expressed in Terms of the Total Volume Fraction of Polystyrene for the Various Blend Systems Investigated

blend systems	$\phi_{Lam,\,Bic}$	$\phi_{Bic,\,Cyl}$
as/s_1	0.305 ± 0.01	0.285 ± 0.01
as/s_2	0.27 ± 0.005	0.245 ± 0.005
as/s_3	0.24 ± 0.005	0.225 ± 0.005
cf. pure SI diblocks and/or blends SI/HS[a]	0.32 ± 0.015	0.28 ± 0.015

[a] The values given for the pure SI diblocks and blends SI/HS were taken from Winey et al. (ref 37).

the various morphologies is highly dependent on the system investigated.

In the approximation of the strong segregation regime, which is qualitatively verified by the analysis discussed in section IV.1, the parameter controlling the phase diagram of pure A−B diblocks[35,37,38] or blends A−B/HA[32b,39] (wet brush regime) is the total volume fraction of A. It should be noted that the composition range is slightly shifted when approaching the order−disorder transition;[38] hence, they are a function of χ as well. However, the differences observed between the three series as/s_i are tremendous and cannot be attributed to the very slight decrease of segregation power

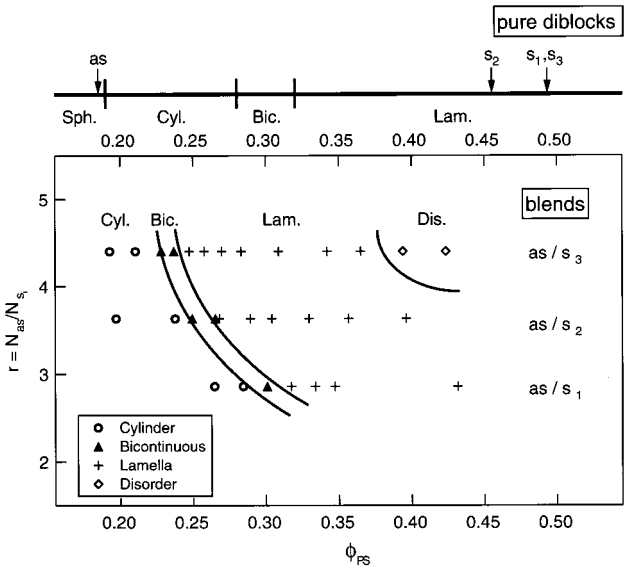

Figure 11. Morphology variation of the blends of two diblock copolymers as/s_i (i = 1, 2, and 3) in the parameter space of $r \equiv N_{as}/N_{s_i}$ and ϕ_{PS}.

when going from as/s_1 to as/s_3. This gives a piece of evidence that, in binary mixtures of two A−B diblocks differing in length and composition, the total volume fraction of A is not the only parameter controlling the morphology. Thus, to try to construct a sort of phase diagram of such mixtures at a constant temperature, a second key parameter must be introduced. To characterize a pair of diblocks $(A-B)_\alpha$ and $(A-B)_\beta$, four parameters are necessary (the length and composition of each diblock). In this work we aimed to focus on the effect of the length of the short symmetric diblock by keeping other three parameters constant. As a second parameter for the phase diagram, we have chosen the ratio between the total degree of polymerization of the long and the short diblock, $r \equiv N_{as}/N_{s_i}$, rather than N_{s_i} alone. Other parameters could be chosen, but it seems intuitive to use N_{as}/N_{s_i} to describe this system where two types of chains differing in length are anchored on the same interface.

Figure 11 shows a phase diagram in the parameter space of r and ϕ_{PS} at a constant temperature. It appears that the morphologies in the ordered phase encountered in the as/s_i mixtures are the classical morphologies of pure A−B diblocks. They are found in the same order, from lamellae to bicontinuous, cylinders, and finally spheres, when decreasing the total volume fraction of PS (ϕ_{PS}). The use of a mixture of two diblocks enables ones to shift significantly the composition range for the different morphologies. The larger the difference in molecular weight between the two diblocks, the larger is the shift.

Therefore, blending diblocks of different molecular weights and compositions is a way to break the interdependence between morphology and volume fracion of A (PS). This effect is intriguing on many aspects. It enables one to investigate the respective effects of composition and morphology on any physical properties, which was not possible up to now. For example, it enables a better understanding of the parameters controlling the viscoelastic properties of block copolymers.[40]

It would be of great interest to investigate how far this effect can be pushed: is it possible to design an SI

mixture having a stable lamellar morphology with a highly asymmetric composition? We can answer that some limits are known already: If the ratio N_{as}/N_{s_i} becomes too large, then the two diblocks are not miscible anymore, and they undergo macrophase separation as it was shown in earlier works.[14]

Looking back to the literature leads us to think that what is observed here on binary mixtures of diblocks could also be true for more complex architectures such as star block copolymers. Indeed, Kraus et al. in 1979[15] investigated polydisperse polystyrene and polybutadiene star block copolymers. They observed that one blend (referenced C in the original paper) which had a volume fraction of polystyrene $\phi_{PS} = 0.75$ had a lamellar morphology. This blend with an unexpected morphology was a blend of two star-block copolymers differing in molecular weights and compositions.

Recently, this shift of the phase boundaries has been described theoretically by Shi and Noolandi[41] as the "cosurfactant effect". On the basis of mean-field calculations, they predicted that in some cases two diblocks differing in molecular weights could segregate with their chemical junctions on the same interface and that the short diblocks would then act as cosurfactants; that is to say, they could induce a shift of the composition range of the morphologies.

Some theoretical works have been dedicated to the understanding of the self-assembly of blends of diblocks in the strong segregation regime.[42] These models deal with the organization of mixed brushes, brushes made of chains differing in length. To investigate the agreement between these models and our experimental results, a detailed analysis of the microdomains sizes is necessary. This will be discussed in the companion paper.[16]

V. Conclusion

This paper is a contribution to the investigation of the self-assembly of block copolymers. The binary mixtures of SI diblocks investigated are miscible at a molecular level; i.e., the two diblocks either self-organize and segregate into a single ordered morphology or remain in a disordered state when the segregation power is not sufficient. In the former case, the fact that competing long-range interactions of the two types of diblocks, differing in molecular weights and compositions, have their junctions segregating on the same interface has a major influence on their morphological behavior. Though the phase diagram is the one found for pure diblocks, the phase boundaries are significantly shifted. This shift increases when the ratio between the chain lengths of the two diblocks increases. Recently, Shi and Noolandi predicted theoretically this phenomenon and described it as a cosurfactant effect.[41] Shifting the phase boundaries of the different morphologies in block copolymers presents several interests, the major one being the opportunity that it provides to investigate separately the effect of composition (volume fraction) and morphology on the materials properties. A better understanding of the physical origin of this phenomenon requires a thorough investigation of the organization of block chains with different lengths within the domains, which will be the topic to be discussed elsewhere.[16]

Acknowledgment. This work was supported in part by a Grant-in-Aid for Scientific Research (under Grant 12305060) from the Ministry of Education, Science and Culture, Japan, and by a Grant from ELF-ATOCHEM (ATOFINA). The authors thank Prof. Lucien Monnerie for encouragements of this work and useful discussions, Dr. Alexander E. Ribbe for a lot of helpful assistance in this TEM work, and Mr. D. Yamaguchi for helpful discussions and assistance in this work.

References and Notes

(1) See for example, a review article: Hashimoto, T. *Thermoplastic Elastomers*, 1st ed.; Legge, N. R., Holden, G. R., Schroeder, H. E., Eds.; Hanser: Vienna, 1987; Chapter 12, Section 3. Hashimoto, T. *Thermoplastic Elastomers*, 2nd ed.; Hanser: Vienna, 1996; Chapter 15A and references therein.
(2) See, for example, a review article: Bates, F. S.; Fredrickson, G. H. *Annu. Rev. Phys. Chem.* **1990**, *41*, 525 and references therein.
(3) Jiang, M.; Xie, H. *Prog. Polym. Sci.* **1991**, *16*, 1006.
(4) Binder, K. *Adv. Polym. Sci.* **1994**, *112*, 182.
(5) Leibler, L. *Macromolecules* **1980**, *13*, 1602.
(6) Matsen, M. W.; Bates, F. S. *Macromolecules* **1996**, *29*, 1091.
(7) (a) Hadziioannou, G.; Skoulios, A. *Macromolecules* **1982**, *15*, 267. (b) Hashimoto, T. *Macromolecules* **1982**, *15*, 1548.
(8) Hashimoto, T.; Tanaka, H.; Hasegawa, H. In *Molecular Conformation and Dynamics of Macromolecules in Condensed Systems*; Nagasawa, M., Ed.; Elsevier: Amsterdam, 1988; p 257.
(9) Koizumi, S.; Hasegawa, H.; Hashimoto, T. *Macromolecules* **1994**, *27*, 4371.
(10) Vilesov, A. D.; Floudas, G.; Pakula, T.; Melenevskaya, E. Y.; Birshtein, T. M.; Lyatskaya, Y. V. *Macromol. Chem. Phys.* **1994**, *195*, 2317.
(11) Spontak, R. J.; Fung, J. C.; Braunfeld, M. B.; Sedat, J. W.; Agard, D. A.; Kane, L.; Smith, S. D.; Satkowski, M. M.; Ashraf, A.; Hajdak, D. A.; Gruner, S. M. *Macromolecules* **1996**, *29*, 4494.
(12) Zhao, J.; Majumdar, B.; Schulz, M. F.; Bates, F. S.; Almdal, K.; Mortensen, K.; Hajdak, D. A.; Gruner, S. M. *Macromolecules* **1996**, *29*, 1204.
(13) Sakurai, S.; Irie, H.; Umeda, H.; Nomura, S.; Lee, H. H.; Kim, J. K. *Macromolecules* **1998**, *31*, 336.
(14) (a) Hashimoto, T.; Yamasaki, K.; Koizumi, S.; Hasegawa, H. *Macromolecules* **1993**, *26*, 2895. (b) Hashimoto, T.; Koizumi, S.; Hasegawa, H. *Macromolecules* **1994**, *27*, 1562.
(15) Kraus, G.; Fodor, L. M.; Rollman, K. W. *Adv. Chem. Ser.* **1979**, *227*.
(16) Court, F.; Hashimoto, T. Manuscript in preparation.
(17) See for example: Mori, K.; Hasegawa, H.; Hashimoto, T. *Polymer* **2001**, *42*, 3009.
(18) Fujimura, M.; Hashimoto, T.; Kawai, H. *Mem. Fac. Eng., Kyoto Univ.* **1981**, *43* (2), 224.
(19) Hashimoto, T.; Suehiro, S.; Shibayama, M.; Saijo, K.; Kawai, H. *Polym. J.* **1981**, *13*, 501.
(20) Suehiro, S.; Saijo, K.; Ohta, Y.; Hashimoto, T. *Anal. Chim. Acta* **1986**, *189*, 41.
(21) Balta-Calleja, F. J.; Vonk, C. G. *X-ray Scattering of Synthetic Polymers*: Elsevier: Amsterdam, 1989.
(22) Hendricks, R. W. *J. Appl. Crystallogr.* **1972**, *5*, 315.
(23) (a) Kato, K. *J. Polym. Sci., Polym. Lett. Ed.* **1966**, *4*, 35. (b) Ribbe, A. E.; Bodycomb, J.; Hashimoto, T. *Macromolecules* **1999**, *32*, 3154.
(24) (a) Pakula, T.; Saijo, K.; Kawai, H.; Hashimoto, T. *Macromolecules* **1985**, *18*, 1294. (b) Hshimoto, T.; Shibayama, M.; Kawai, H.; Meier, D. J. *Macromolecules* **1985**, *18*, 1855. (c) Balsara, N. P.; Perahia, D.; Safinya, C. R.; Tirrell, M.; Lodge, T. P. *Macromolecules* **1992**, *25*, 3896.
(25) Hajduk, D. A.; Harper, P. E.; Gruner, S. M.; Honeker, C. C.; Kin, G.; Thomas, E. L.; Fetters, L. J. *Macromolecules* **1994**, *27*, 4063.
(26) Wiener, O. *Abh. Math.-Phys. Kl. Saechs. Ges. Wiss.* **1912**, *32*, 507.
(27) Shibayama, M.; Hashimoto, T. *Macromolecules* **1986**, *19*, 740.
(28) Sakamoto, N.; Hashimoto, T. *Macromolecules* **1995**, *28*, 6825.
(29) The Bragg spacing $D = 2\pi/q_m$ for the bicontinuous domain structure is ~30 nm, which is roughly comparable with thickness of the ultrathin sections (40−50 nm). Thus, an artifact brought by an overlapping of the image along the thickness direction will not significantly affect our interpretation on the connectivity of the PS domain in 3D space. The quality of the TEM images appeared to be low because of

small grains with varying orientation. However, this reflects nature of order that these blends have.

(30) Lin, E. K.; Gast, A. P.; Shi, A.-C.; Noolandi, J.; Smith, S. D. *Macromolecules* **1996**, *29*, 5920.

(31) Yamaguchi, D.; Bodycomb, J.; Koizumi, S.; Hashimoto, T. *Macromolecules* **1999**, *32*, 5884.

(32) (a) Hashimoto, T.; Tanaka, H.; Hasegawa, H. *Macromolecules* **1990**, *23*, 4378. (b) Tanaka, H.; Hasegawa, H.; Hashimoto, T. *Macromolecules* **1991**, *24*, 240. (c) Tanaka, H.; Hashimoto, T. *Macromolecules* **1991**, *24*, 5713.

(33) Thomas, E. L.; Alward, D. B.; Kinning, D. J.; Martin, D. C.; Handlin, D. L.; Fetters, L. J. *Macromolecules* **1986**, *19*, 2197.

(34) Kinning, D. J.; Thomas, E. L.; Alward, D. B.; Fetters, L. J.; Handlin, Jr., D. L. *Macromolecules* **1986**, *19*, 1288.

(35) Hasegawa, H.; Tanaka, H.; Yamasaki, K.; Hashimoto, T. *Macromolecules* **1987**, *20*, 1651.

(36) Winter, H. H.; Scott, D. B.; Gronski, W.; Okamoto, S.; Hashimoto, T. *Macromolecules* **1993**, *26*, 7236.

(37) Winey, K. I.; Gobran, D. A.; Xu, Z.; Fetters, L. J.; Thomas, E. L. *Macromolecules* **1994**, *27*, 2392.

(38) Khandpur, A. K.; Förster, S.; Bates, F. S.; Hamley, I. W.; Ryan, A. J.; Bras, W.; Almdal, K.; Mortensen, K. *Macromolecules* **1995**, *28*, 8796.

(39) Winey, K. I.; Thomas, E. L.; Fetters, L. J. *Macromolecules* **1992**, *25*, 2645.

(40) Court, F.; Monnerie, L.; Hashimoto, T., to be submitted.

(41) Shi, A.-C.; Noolandi, J. *Macromolecules* **1994**, *27*, 2936. Shi, A.-C.; Noolandi, J.; Hoffmann, H. *Macromolecules* **1994**, *27*, 6661. Shi, A.-C.; Noolandi, J. *Macromolecules* **1995**, *28*, 3103.

(42) Birshtein, T. M.; Liatskaya, Y. V.; Zhulina, E. B. *Polymer* **1990**, *31*, 2185. Zhulina, E. B.; Birshtein, T. M. *Polymer* **1991**, *32*, 1299. Zhulina, E. B.; Lyatskaya, Y. V.; Birshtein, T. M. *Polymer* **1992**, *33*, 332. Lyatskaya, J. V.; Zhulina, E. B.; Birshtein, T. M. *Polymer* **1992**, *33*, 343. Birshtein, T. M.; Lyatskaya, Y. V.; Zhulina, E. B. *Polymer* **1992**, *33*, 2750.

MA001314+